

Numerical Simulation of the Dynamic Breakage Characteristic of African Norite

P.Vanichkobchinda^{1*}, D.J. Reddish², L.R. Stace² and D.N. Whittles³

¹ School of Engineering, University of the Thai Chamber of Commerce, Bangkok, 10400, Thailand

² School of Civil Engineering, University of Nottingham, University Park, Nottingham, NG7 2RD, UK

³ Arup, Arup campus, Blythe Gate, Blythe Valley-ark, Solihull, B90 8AE, UK

Abstract

Laboratory drop weight tests rig and numerical modelling have been used to investigate the impact energy effect on the degree of dynamic fragmentation of cylindrical rock samples. The drop weight tests indicated that the degree of dynamic fragmentation of the African Norite formed a non-linear relation with impact energy. In the numerical modelling of the drop weight test, the shear localisation developed in the African Norite was assumed to represent discrete fracture planes. Shear bands, outputs of the image analysis of the numerical model, were used to separate solid material from shattered or broken material, allowing the FLAC output from the dynamic modelling to be processed into black and white fragmented images. This was undertaken to determine particle size distributions. Corresponding grading curves from the numerical modelling were then validated against the laboratory derived curves indicating the potential of numerical modelling to simulate the process of rock fragmentation.

Keywords: Numerical modeling; Rock fragmentation; Crushing; Energy; African Norite; Photography

1. Introduction

The dynamic fragmentation of rock materials is a fundamental activity that lies at the start of many manufacturing in mining industrial, especially in size reduction processes [1,2,3].

The present research has been conducted with a view to improving the understanding of the basic impact breakage process, allowing it to be simulated more accurately. By improving the simulation of breakage in numerical models it should be possible to optimise the fragmentation process in terms of energy input and of product size for a wide range of crushing processes.

* Corresponding author.
E-mail : pongtana@utcc.ac.th

Recently, Reddish et al. and Pongtana et al. [2,4] have been conducted with a view to improve the understanding of the basic impact breakage process, allowing it

to be simulated more accurately. By improving the simulation of breakage in numerical models it should be possible to optimise the fragmentation process in terms of both energy input and product size range produced for a wide range of rock fragmentation processes in to the medium to soft rock, which are Cornish Grey Penryn Granite and Daley Dale Sandstone. Other authors have studied the dynamic fragmentation process in a number of contexts. General dynamic fragmentation papers are presented by a range of authors [5-12]. Rock crushing is addressed in papers [13-17], rock cutting in [18] and blasting in papers [19- 22].

Therefore, this experimental procedure adopted is to use an impact rig to dynamically load cylindrical specimens of very hard rock and then measure the resulting fragmentation by sieving of the fragmented product. The tests were also photographed using high speed photography to study order of fracturing. Sequences of tests have been conducted for different impact masses and impact velocities. The experimental results have been used to validate a numerical simulation of the same process using the finite difference approach. The numerical model includes a number of innovations, most notably a methodology to fragment and size the impacted sample [2,4].

2. Laboratory Drop Weight Testing and Size Analysis

2.1. The Drop Weight Test

The drop weight testing machine is a useful tool to determine the energy input/size reduction relation for breakage of brittle materials. Its use has dramatically increased in recent years for evaluating breakage parameters of various forms [23,24]. The key controlling parameter of drop weight testing is the input energy [2,4]. This is determined from the mass of the drop weight and the distance through which it falls prior to impacting the sample using Eq. (1).

$$E = mgs, (1)$$

where

E =energy (joules), m =mass of sample (kg), g =gravitational acceleration (9.81m/s²) and s =drop height (m).

Samples had a diameter of 37.5mm and a height of 75mm and were prepared in accordance with the ISRM standards for uniaxial compressive testing [25]. The samples were dynamically loaded along their long axis with direct contact being made between the travelling hardened steel platen and stationary flat topped sample.

The drop weight tests were conducted on the prepared cylindrical samples at three drop weight increments of 30, 40 and 50 kg and three height increments of 600, 800 and 1000 mm, respectively. The impact energy in joules for each of these configurations is given in Table 1. For each configuration of drop height and weight five samples were tested.

Table 1 Impact energy (joules) for the drop weight test

Drop Weight (kg)	Drop Weight (mm)		
	600	800	1000
30	177	235	294
40	235	314	392
50	294	392	491

2.2. Sieve Size Analysis

After each test the broken sample was removed from the machine and sieved to determine the size distribution. The sieve sizes used were in two ranges:

- 37.50, 31.50, 26.50, 22.40, 19.00, 13.20, 9.50, 6.70, 4.75, 3.35 mm, and
- 2.36, 1.70, 1.18, 0.850, 0.600, 0.425, 0.300 mm.

The cumulative frequency size distribution curves for constant drop weights are given in Figure 1. The Figures show, as would be anticipated, that with increasing energy of impact a greater degree of fragmentation of the African Norite samples occurs. This experimental result has been used to validate a numerical simulation of the same process using the finite difference approach.

3. Numerical Modelling

Numerical modelling of drop weight testing on African Norite, samples was conducted utilising a commercial two dimensional finite difference code developed for geomechanical problems known as FLAC

The FLAC numerical modelling software was used in full dynamic mode so that the correct energy balance required to simulate fragmentation was maintained. The dynamic simulation also allowed the impact forces, strain rates and propagation of stress waves within the medium.

The model was constructed in three representative parts: the drop weight, the rock sample and the underlying anvil. The finite difference grid generated by FLAC. The finite difference grid of the drop weight, the African Norite and the bottom anvil was divided into 69056 elements and each element size was represented to be 0.5 mm wide by 1 mm high. The grid which was graded horizontally with distance from one end of rock sample to the others, is shown in Figure 2. [2,4]

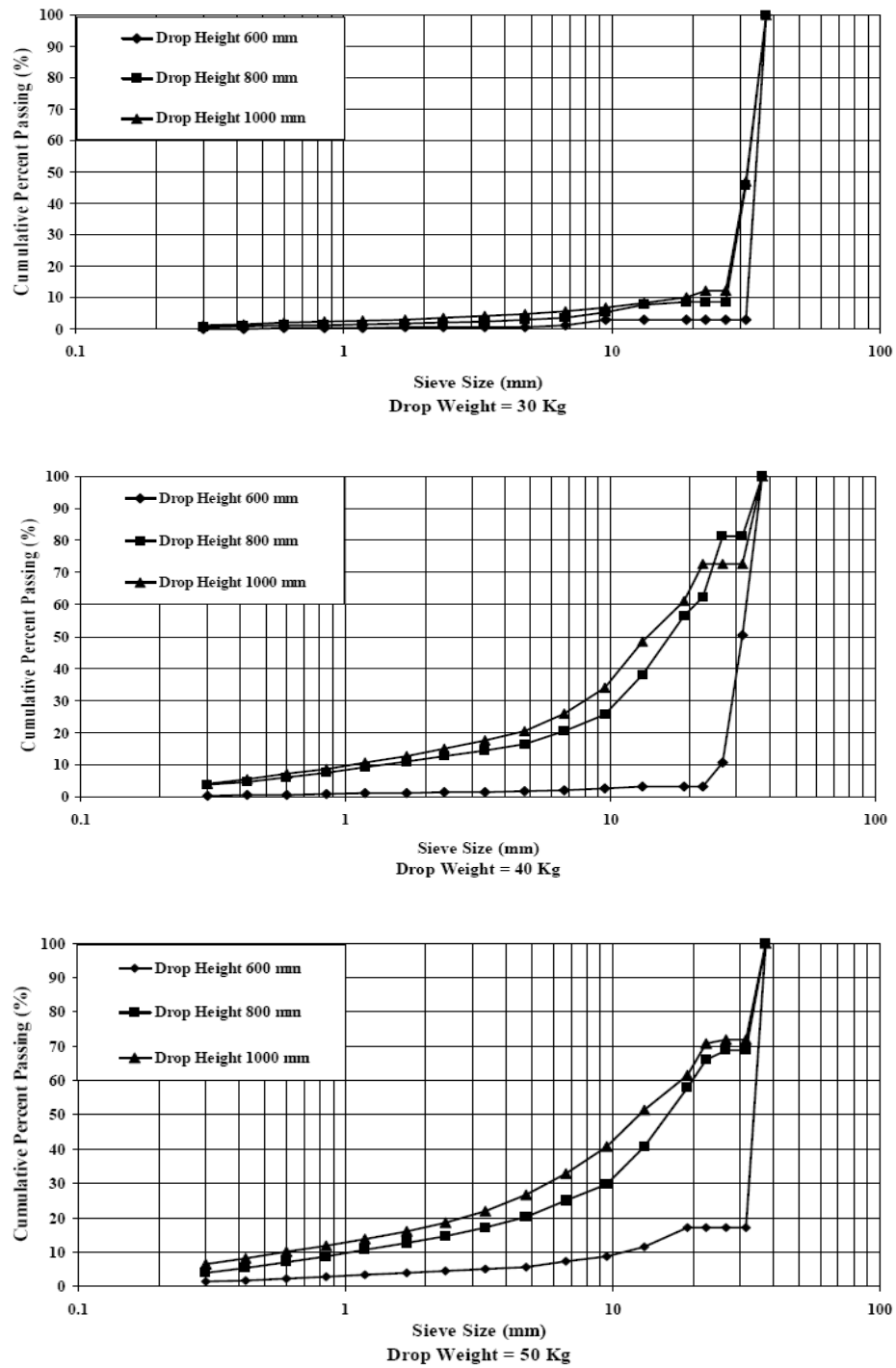


Fig. 1. Cumulative frequency size distribution curves with constant drop weight of 30, 40 and 50 kg. for African Norite.

3.1. Modelling of the Contact Surface between the Sample, the Drop Weight and Bottom Anvil

Interfaces used to model the contact between the drop weight and sample, and the bottom anvil and sample, is shown in Figure 2. The interfaces were prescribed by normal and shear stiffness. The normal stiffnesses of the interfaces were set to high values in relation to the surrounding medium to simulate a hard contact surface.

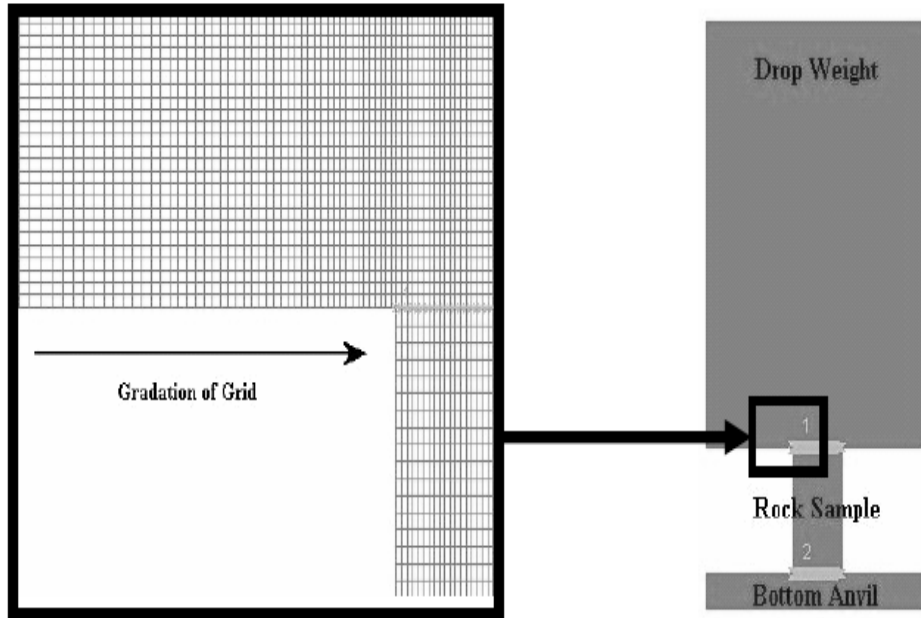


Fig. 2. Finite difference modelling of drop weight testing set and rock sample

3.2. Two Dimensional Correction

The FLAC modelling was undertaken as a two-dimensional plane strain analysis for a number of practical reasons. Given that the main thrust of this research was to study fragmentation and process its results into size distributions the complexity of processing three-dimensional results into three-dimensional objects and then sizing these objects was seen as too ambitious at this stage in the study. However, it will only compare two-dimensional sections through the model and is unlikely to attempt to analyse three dimensional fragments. The image analysis software utilised later in the results analysis is strictly limited to two-dimensions. The development of three-dimensional fragment processing and sizing software would require considerable additional effort and resources in its own right. A logical compromise is to initially conduct a two-dimensional analysis to improve understanding at this level before attempting the far more complex three-dimensional analysis.

To correct the two-dimensional representation of the three-dimensional drop weight test, adjustment of the material properties was required. The correction used a reduction factor based on an equivalent volume approach [2,4,25,26]. The equivalent volume value was determined using Eq. (2)

$$EV = V_a/V_m \quad (2)$$

where EV is the equivalent volume value, V_a is the actual volume of the material, and V_m is the volume of the material in the 2D representation.

The stiffness, density, cohesion and tensile strength material parameters were reduced within the model by multiplying the actual values by EV . Two materials need to be simulated within the model of the drop weight test. These are the African Norite sample, which is capable of brittle failure and yield, and the robust steel structure of the testing system (drop weight and anvil).

3.3. Laboratory Testing

The mechanical properties of rock materials required in computer simulation analysis known as Fast Lagrangian Analysis of Continua (FLAC) [27], are generally categorized in one of two groups, elastic deformability properties and strength properties. Selection of appropriate and realistic properties is often the difficult element in the generation of a model because of the high degree of uncertainty in the properties of rock caused by its natural formation. When performing a numerical analysis especially, in the field of Geomechanics, it should be noted that the problem will always involve a data-limited system. However, with the appropriate selection of properties based upon the available data, important insights into the physical problem can still be gained.

Laboratory testing of the African Norite was undertaken to determine its Young's Modulus, unconfined compressive strength, Brazilian Disc tensile strength and triaxial strength. The unconfined and triaxial testing was undertaken on cylindrical core samples, similar to those used in the drop weight test, using a servo-controlled stiff press with lateral confinement being provided by a Hoek Cell. The axial deformation of the samples was measured during the unconfined compression tests using two LVDT's to allow determination of the Young's Modulus. All the testing was undertaken in accordance with ISRM standard procedure.

In this research, the Mohr-Coulomb and the Hoek-Brown criteria are applied to the rock material strength properties subjected to dynamic loading and [28] indicated that rock material strength under dynamic loading can be approximately described by the Mohr-Coulomb criterion, at low confining pressure range. The change of strength is primarily due to the variation of cohesion with loading rate. The rock material strength under dynamic loads is better described by Hoek-Brown criterion. Assessment of the Hoek-Brown criterion shows that the uniaxial compressive strength increases with increasing loading rate, and the parameter m_i value appears

unaffected by the loading rate. Therefore, the strength properties were determined from the test data by fitting a non-linear Hoek–Brown failure criterion [29]. The material parameter, m_i , in this function was calculated, by non-linear least squares regression, as having a value of 17.9. The numerical modelling indicated that the minimum principal stress magnitudes experienced by the samples during the drop weight test would be in the range of tensile to very low confinement. Therefore the failure criterion was used to determine an average friction and cohesion value over this range of minimum principal stress experienced by the sample during the drop weight test (10 MPa in tension to 1 MPa compression). The parameters used to represent the African Norite are given in Table 2.

To represent the constitutive behaviour of the African Norite, a Mohr–Coulomb strain–softening material model was adopted. To simulate the brittle fracture of the African Norite, the strength was reduced to the residual value (fracture strength) given in Table 2 at a small amount of plastic strain.

Table 2
Material Properties of the African Norite

<i>Elasticity Properties</i>		
—Bulk modulus		24.93 GPa
—Shear modulus		18.04 GPa
—Density		2876 kg/ m ³
<i>Hoek–Brown Strength parameters (Peak)</i>		
— m_i		17.9
— s		1
<i>Mohr–Coulomb Strength parameters</i> (averaged over σ_3 range—10 to 1MPa)		
Peak strength	Friction angle	65.6°
	Cohesion	22.9 MPa
	Tensile strength	10.4 MPa
Residual strength	Friction angle	65.6°
	Cohesion	0 MPa
	Tensile strength	0 MPa

One of the initial objectives of this study by comparing laboratory impact breakage results to numerical models was to determine if static properties and failure criteria were appropriate for modelling dynamic breakage at the loading rates typically developed in the test apparatus. The initial criteria and methodology chosen have proven satisfactory to date producing reasonably realistic results with little correction or modification. However, further detailed parametric study may eventually indicate that changes are required to failure criteria to model the dynamic failure optimally [30]. The authors also have good quality high speed camera images of the breakage sequence of test samples. The sequences are timed and would allow detailed fracture development. The authors are also working on alternative heterogeneous numerical models of other types of rock tested where the granular nature of the samples is taken into account.

3.4. Modelling of the Steel Drop Weight and Anvil

The steel structure (drop weight head and anvil) of the drop rig system was simulated as a linear elastic material with no yield. A representative Young's Modulus for the mild steel structure was taken to be 200 GPa with a Poisson's Ratio of 0.3 [31].

3.5. Modelling Procedure

To monitor the stress wave [32], due to the impact, as it was transmitted through the sample, histories were recorded of the vertical stress at nine locations within the sample. The model stress wave takes approximately 4000 time steps from the moment of impact to pass through the entire sample. This indicated that the model must be run for at least this number of timesteps after impact to simulate the full effect of the drop weight test.

3.6. Development of Methodology for Fragmentation Analysis of Numerical Models

During brittle fracturing and failure of rock, there is a complicated progressive failure process which is characterized by coalescence of micro-fracture growth. This demonstrates stress distribution from failure in rock elements leading to post peak to form discrete microscopic fracture propagation [11]. In order to simulate the effects of the fundamentals of fracture mechanism processes within a numerical model, it is often assumed that it is possible to capture the influence of the micro-mechanisms by distributing them uniformly into the area, which is populated a set of discrete fracture [39]. It is generally considered that the crack density increases with spatial clustering of cracks at peak stress and shear localisation in the strain softening stage [40]. In the computer simulations of the drop weight test the shear localisation within the material that developed into distinctive shear bands was used to predict the fracture pattern of the Norite.

Shear strain localisation is simulated within the FLAC models at the onset of yield and progressively develops during subsequent strain softening. This allows the FLAC models to simulate crack propagation within the material. Previous research had also indicated that shear strain contours within FLAC models can be strongly correlated with areas of fracturing encountered in a range of rock mechanics modelling problems.

3.7. Image Analysis

In the modelling exercise shear bands were used to separate solid material from shattered or broken material, allowing the FLAC output from the dynamic modelling to be processed into black and white fragmented images. To determine the magnitude of the shear strain increment that represented the full development of macroscopic fracture planes, sequences of images were constructed at 7.5, 10 and 12.5 mm/m shear strain increments, which recommended by Pongtana et al. and reddish et al.

These images were then analysed using the image analysis software, Image Tool for Windows Version 3.00 [35]. The image analysis program identified each zone separated by a contiguous white band, which represented shear strain of greater than the prescribed limit. The black zones were considered to represent a discrete fragment. The white zones were not included in the image size analysis. For each identified black fragment, the software determined the dimensions of the shortest axis of that fragment and also the area of the fragment. The short axis dimension was considered to represent the dimension that determined the sieve size that the fragment could pass through.

In this research work, for each identified black fragment the software determined the dimensions of the shortest axis of that fragment according to recommendation of Reddish et al. [2], Pongtana et al [4], Banta et al. [42], Xu [43]. The selected method of dimensional analysis is LBRW: Least Bounding Rectangle Width, LBRL: Least Bounding Rectangle Length. The short axis dimension (LBRW) was considered to represent the dimension that determined the sieve size that the fragment could pass through. The simulated grading curves generated from the FLAC models of constant drop height of 1000mm and for constant drop weight of 50 kg in Figure 3 and 4.

Grading curves were constructed for shear strain increments of 7.5, 10 and 12.5 mm/m and the corresponding grading curves obtained for the fracture pattern compared to the actual grading curves obtained by sieving. From this exercise the 10 mm/m shear strain increment was determined as providing the best fit size distribution to the actual test data and was identified as the key value in delineating fracture. In fact other data concerning failure mode and other output data tend to confuse the situation rather than clarifying it. The static failure criteria utilised in this study have proven reasonably accurate in delineating fracture behaviour. However, although the shear strain fracture criterion's influence has been studied across a range of values, a systematic variation of the fundamental failure criteria used in the model needs to be undertaken. This becomes particularly important if the modelling is to be extended outside of the loading rate range covered in this drop testing.

3.8. Results of the Modelling of the Drop Weight Test

Figure 3 shows a similar sequence of fracture images for a shear strain increment of 10 mm/m. In this case the constant drop weight of 50 kg was applied with drop heights of 600, 800 and 1000 mm. Again the fracture images clearly illustrate the increased fragmentation with increasing drop height.

The grading curves shown in Figure 8 indicate a clear trend in product size changes with both sequences which can be correlated with the impact energy of the drop weight.

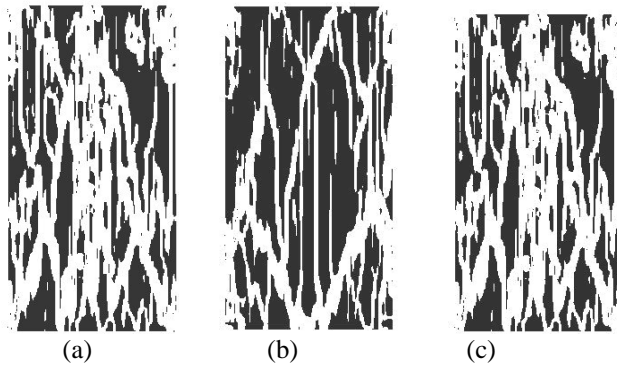


Fig. 3. Fracture pattern of modelling of African Norite analysed by image analysis technique with 10 mm/m shear strain increment cut point. Constant drop weight of 30 kg with drop height of 600 mm for (a), 800 mm for (b) and 1000 mm for (c). with 10mm/m shear strain increment cut point.

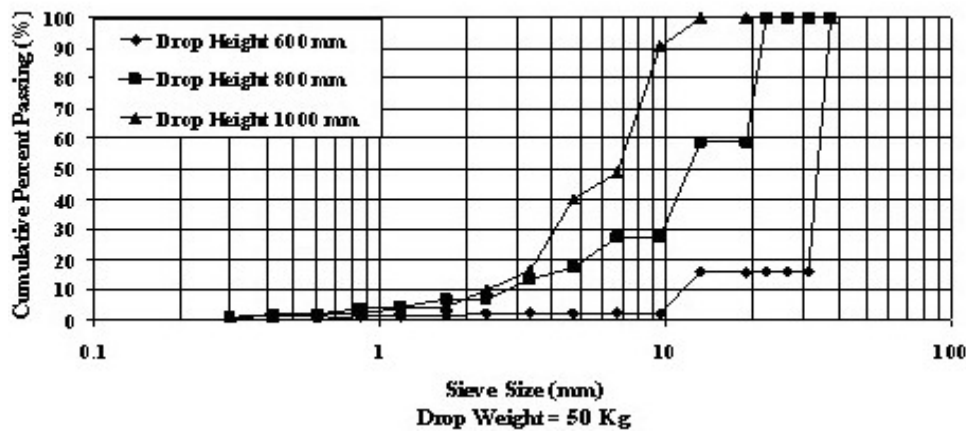


Fig. 4. Cumulative frequency size distribution curves with constant simulated drop weights of 50 kg. for African Norite.

4. High Speed Camera Recording Technique

The experimental study was conducted to investigate the fracture process of cylindrical rock specimens under impact. In this experiment, an Imacon-486 high speed framing camera (200,000,000 frames/sec) was used to record the fracture propagation during the fracture process in the drop weight test. The fracture propagation patterns were compared with the fracture patterns obtained using the two dimensional finite difference code (FLAC). Computer-generated crack patterns were presented and compared to experimentally observed crack patterns in the fracture of rock. The high speed camera set is shown in figure 5. The result of fracture propagation is shown in Figure 6.



Fig. 5. High speed camera set

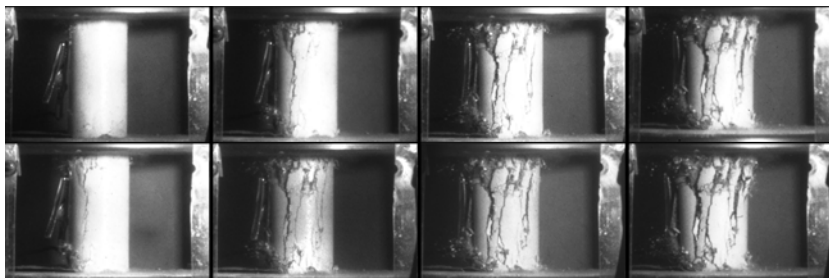


Fig. 6. Pattern of fracture propagation of African Norite recorded by high speed camera

5. Comparison of Models with Laboratory Tests

Grading curves using the procedure described above were constructed for the numerical simulations representing the drop weight tests with a weight of 50 kg and drop heights of 600, 800 and 1000 mm. The comparisons between these numerical modelling simulations and the actual drop weight test results are shown in Figure 9. It can be seen from the figures that in general, the numerical simulations produce a curve which closely corresponds to the curve produced for the finer fraction from the tests up to the sieve size corresponding to approximately 60-80% passing. The prediction of the very fine and coarser fraction size distribution is not as close. This is due to the nature of the image analysis which only identifies particles with a contiguous band of shear. In the analysis, very fine fraction size was deleted by image increasing of the thickness of shear band while if two discrete particles were connected only by one pixel, the two particles would be combined for coarser grain thus affecting the size distribution of the grading curve.

A series of drop weight tests have been undertaken on cylindrical specimens of Norite at nine different drop height/weight configurations. The degree of fragmentation of each sample has been represented by the sieve sizes that 25%, 50% and 75 % of the broken sample would pass through. The degree of fragmentation has been shown to be linearly inversely related to impact energy.

The Norite was by far the strongest rock type tested and even during the drop tests there were problems with delivering enough energy to the samples to ensure breakage. Ideally larger weights and drop heights would have been available for the Norite tests. For this reason the FLAC model development for Norite was halted and ongoing development effort was concentrated on the other rock types. To conclude the basic homogeneous model has failed to simulate the Norite as well as would be ideal.

The computer numerical modelling program FLAC has been utilised to simulate the drop weight test on the homogeneous modelling of Norite sample. The output of the model was analyzed in terms of shear strain banding within the sample. Image analysis on outputs obtained from the FLAC modelling was undertaken to determine the particle dimensions allowing simulated grading curves to be constructed. The grading curves showed that the optimum shear strain increment to predict macroscopic fracture planes was 10 mm/m.

The simulated grading curves obtained from FLAC modelling and image analysis were compared to the corresponding grading curves obtained from the laboratory drop weight test. The comparison indicated that the FLAC modelling provides a method of predicting the dynamic fragmentation of the cylindrical Norite samples. However, from the analysis it can be seen that FLAC has limited capabilities in predicting the size of smaller and larger single broken particles, from the finer and coarser fraction. In the image analysis program, the area of a particle is represented by a number of pixels. Should two big particles be connected to each other in the model by just one pixel, the image program would represent this as one piece. In reality, in the actual size reduction process, the particle would be broken. Additionally the shear zones interpreted as fractures are relatively wide due to element size and other issues. In practice these shear zones would be narrow cracks with little or no volume.

The aim of this study was to test a homogeneous numerical model fragmentation methodology on a sequence of measured laboratory breakage tests. The simulation has proven to be realistic and shows promise for further development. By validating the numerical modelling approach on the laboratory drop rig experiment, its use on more realistic industrial breakage processes becomes a possibility. It is envisaged that a validated fragmentation model for a rock type could be used in a series of simulations to optimise the operational parameters of plant such as crushers at the design stage.

For the future work, the numerical simulation model of dynamic rock fragmentation is needed on the constitutive FLAC model to simulate cracks as more realistic rock narrow separations rather than wide shear zones. Additionally the image analysis program needs to be developed address some of the issues raised by larger particle.

References

1. Zhao J., Li H.B., Wu M.B., Li T.J. Dynamic Uniaxial Compression Test on a Granite, *International Journal of Rock Mechanics and Mining Sciences*. 1999;36:273–277.
2. Reddish D.J., Stace L.R., Vanichkobchinda P., Whittles D.N. Numerical Simulation of the Dynamic Impact Breakage Testing of Rock, *International Journal of Rock Mechanics and Mining Sciences*. 2005;42(2):167–176.
3. Whittles D.N., Kingman S., Lowndes I., Jackson K. Laboratory and Numerical Investigation into the Characteristics of Rock Fragmentation, *Mineral Engineering*. 2006;19:1418– 1429.

4. Vanichkobchinda P., Reddish D.J., Stace L.R., Whittles D.N. Numerical Simulation of the Dynamic Breakage Testing of Sandstone, Part I: Development of Homogeneous Constitutive Model for the Fragmentation Analysis in Sandstone, *International Journal of Material & Structure Reliability*, 2007;5(1): 29-44.
5. Mishnaevsky L.L., Physical Mechanisms of Hard Rock Fragmentation under Mechanical Loading, *International Journal of Rock Mechanics and Mining Sciences & Geomechanics Abstract*. 1995;32(8):763-766.
6. Grady D.E., Kipp M.E. Dynamic Rock Fragmentation. In: Atkinson BK editor. *Fracture Mechanics of Rock*. London: Academic Press; 1991.
7. King R.P., Bourgeois F. Measurement of Fracture Energy during Single - Particle Impact Fracture, *Mineral Engineering*. 1993;6(4):353-367.
8. Rizk A.M.E., El-Saggeer H.A.A., Doheim M.A. Examination of Single and Repetitive Impact Breakage, *Mineral Engineering* 1994;6(4): 479-490.
9. Li C., Richard P., Nordlund E. The Stress-Strain Behaviour of Rock Material Related to Fracture under Compression, *Engineering Geology*. 1998;49:293-302.
10. Tang C.A., Kaiser P.K. Numerical Simulation of Cumulative Damage and Seismic Energy Release during Brittle Rock Failure—Part I: Fundamental, *International Journal of Rock Mechanics and Mining Sciences*. 1998;35(2):113-121.
11. Li H.B., Zhao J., Li T.J. Micromechanical Modelling of the Mechanical Properties of a Granite under Dynamic Uniaxial Compressive Loads, *International Journal of Rock Mechanics and Mining Sciences*. 2000;37:923-935.
12. Zhang Z.X., Kou S.Q., Jiang L.G., Lindqvist P.A. Effects of Loading Rate on Rock Fracture: Fracture Characteristics and Energy Partitioning, *International Journal of Rock Mechanics and Mining Sciences*. 2000;37:745-762.
13. Li G., Xu X. Experimental Investigation of the Energy-Size Reduction Relationship in Comminution using Fractal Theory, *Mineral Engineering* 1993;6(2):163-172.
14. Kapur P.C., Pande D., Fuerstenau D.W. Analysis of Single-Particle Breakage by Impact Grinding, *International Journal of Mineral Processing*. 1997;49:223-236.
15. Thomas A., Filippov L.O. Fractures, Fractals and Breakage Energy of Mineral Particle, *International Journal of Mineral Processing* 1999;57:285-301.
16. Tang C.A., Liu H., Lee P.K.K., Tsui Y., Tham L.G. Numerical Studies of the Influence of Microstructure on Rock Failure in Uniaxial Compression—Part I: Effect of Heterogeneity, *International Journal of Rock Mechanics and Mining Sciences*. 2000a;37:555-569.
17. Tang C.A., Tham L.G., Lee P.K.K., Tsui Y., Liu H. Numerical Studies of the Influence of Microstructure on Rock Failure in Uniaxial Compression—Part II: Constraint, Slenderness and Size Effect, *International Journal of Rock Mechanics and Mining Sciences*. 2000b;37:571-583.
18. Liu H., Kou S.Q., Lindqvist P-A. Numerical Simulation of the Fracture Process in Cutting Heterogeneous Brittle Material, *International Journal for Numerical and Analytical Methods in Geomechanics*. 2002;26:1253-1278.
19. Shockey D.A., Curran D.R., Seaman L., Rosenberg J.T., Petersen C. Fragmentation of Rock under Dynamic Loads, *International Journal of Rock Mechanics and Mining Sciences & Geomechanics Abstract*. 1974;11:303-317.
20. Cho S.C., Nishi M., Yamamoto M., Kato M., Kaneko K. Estimation of Rock Fragmentation in Bench Blasting using Numerical Simulation, *Proceedings of the Conference on Explosives and Blasting Technique*. 2002;1:187-196.
21. Cho S.H., Nishi M., Yamamoto M., Kaneko K. Fragment Size Distribution in Blasting. *Material Transactions* 2003a;44(5):951-956.
22. Chu K.T., Wu S.Z., Zhu W.C., Tang C.A., Yu T.X. Dynamic Fracture and Fragmentation of Spheres, 16th ASCE Engineering Mechanics Conference, University of Washington, Seattle, July 16-18, 2003.
23. Zhang Y.Q., Hao H., Lu Y. Anisotropic Dynamic Damage and Fragmentation of Rock Materials under Explosive Loading, *International Journal of Engineering Science* 2003;41:917-929.
24. Tavares L.M. Energy Absorbed in Breakage of Single Particles in Drop Weight Testing, *Mineral Engineering*. 1999;12(1):43-50.
25. Brown E.T. editor, *Suggest Methods for Determining the Uniaxial Compressive Strength and Deformability of Rock Material and Rock Characterisation. Testing and Monitoring: ISRM Suggested Methods*. Oxford: Pergamon Press; 1981.
26. Swift G.M. An Examination of Stability Issues Relating to Abandoned Underground Mine Working, Ph.D. thesis, University of Nottingham, UK, 2000.
27. Itasca Consulting Group 2000, *Fast Lagrangian Analysis of Continua (FLAC) User's Guide*, Version 4, Itasca Consulting Group Inc, Minneapolis, Minnesota, USA, 2000.
28. Zhao J. Applicability of Mohr-Coulomb and Hoek-Brown Strength Criteria to the Dynamic Strength of Brittle rock, *International Journal of Rock Mechanics and Mining Sciences*. 2000;37:1115-1121.
29. Hoek E., Kaiser P.K., Bawden W.F. *Support of Underground Excavations in Hard Rock*. Rotterdam: Balkema; 1995.
30. Cho S.H., Yuji O., Kaneko K. Strain-rate dependency of the dynamic tensile strength of Rock, *International Journal of Rock Mechanics and Mining Sciences*. 2003b;40:763-777.
31. Kuzmanovic BO, Willems N. *Steel Design for Structural Engineers*. New Jersey: Prentice-Hall; 1977. p. 27-33.

32. Donzé F.V., Bouchez J., Magnier S.A. Modelling fracture in rock blasting, *International Journal of Rock Mechanics and Mining Sciences*. 1997;34(8):1153–1163.
33. Kuijpers J.S., Napier J.A.L. Effective Growth Rules for Macro Fracture Simulation in Brittle Rock under Compression, Eurock'96, Balkema, Rotterdam.
34. Wu X.Y., Baud P., Wong T. Micromechanics of Compressive Failure and Spatial Evolution of Anisotropic damage in Darley Dale Sandstone, *International Journal of Rock Mechanics and Mining Sciences* 2000;37:143–160.
35. Wilcox D., Dove B., McDavid D., Greer D. UTHSCSA Image Tool for Windows Version 3. The University of Texas Health Science Center in San Antonio USA, 2002.
36. Banta L., Cheng K., Zaniwski J. Estimation of Limestone Particle Mass from 2D Images, *Powder Technology*. 2003;132: 184–189.
37. Xu R., Andreina O., Di Guida A. Compression of Sizing Small using Different Technologies, *Power Technology*. 2003;132: 145–153.